ISBN: 978-3-95450-204-2 ISSN: 2673-5350 doi:10.18429/JACoW-IBIC2019-TUPP034

ANALYSIS OF QUADRUPOLAR MEASUREMENTS FOR BEAM SIZE DETERMINATION IN THE LHC

D. Alves*, M. Gasior, T. Lefèvre, CERN, Geneva, Switzerland

Abstract

Due to limitations with non-invasive beam size diagnostics in the LHC, particularly during the energy ramp, there has been an interest to explore quadrupolar-based measurements for estimating the transverse beam size, and hence determining the transverse emittance. This technique is especially attractive as it is completely passive and can use the existing beam position instrumentation. In this work, we perform an analysis of this method and present recent measurements taken during energy ramps. Quadrupolar-based measurements are compared with wire-scanner measurements and a calibration strategy is proposed to overcome present limitations.

INTRODUCTION

Recently, there has been a rising interest in exploring the capabilities of existing beam position instrumentation for estimating transverse beam sizes in the LHC. These measurements are in fact very challenging in the LHC mainly due to the low relative sensitivity ($\approx 10^{-3}$ mm^{-2}) of the existing Beam Position Monitors (BPMs) to the quadrupolar moment. BPM systems equiped with the high resolution Diode ORbit and OScillation (DOROS) electronics [1] have therefore been used. These systems are based on diode detectors with limited dynamic range. For this reason, the DOROS electronics makes use of a set of amplification stages with automatic gain adjustments ensuring that the diodes always operate in their linear regime [2].

Recently, encouraging results with this technique have been presented in [3] and [4]. In this work, we present a different approach for the absolute estimation of the transverse beam sizes, based on the cross-calibration of the various BPM systems against Wire-Scanner (WS) measurements.

PHYSICS

In the case of Gaussian-like transverse beam profiles, the quadrupolar moment Q is defined by [5]:

$$Q = Q_\sigma + Q_r = \left(\sigma_\mathrm{H}^2 - \sigma_\mathrm{V}^2\right) + \left(x^2 - y^2\right) \tag{1}$$

where $\sigma_{\mathrm{H,V}}$ represent the RMS horizontal and vertical transverse beam sizes, x and y represent, respectively, the horizontal and vertical average beam positions, $Q_\sigma = \sigma_\mathrm{H}^2 - \sigma_\mathrm{V}^2$ and $Q_r = x^2 - y^2$.

* diogo.alves@cern.ch

Taking the usual multipole expansion of BPM amplitudes [5] we get, for each electrode:

$$H_1 = h_1 I\left(c_{0h} + c_{1h}x + c_{2h}Q + \ldots\right) + k_1 \tag{2}$$
$$H_2 = h_2 I\left(c_{0h} - c_{1h}x + c_{2h}Q + \ldots\right) + k_2 \tag{3}$$
$$V_1 = v_1 I\left(c_{0v} + c_{1v}y - c_{2v}Q + \ldots\right) + w_1 \tag{4}$$
$$V_2 = v_2 I\left(c_{0v} - c_{1v}y - c_{2v}Q + \ldots\right) + w_2 \tag{5}$$

where I is the beam intensity, the c coefficients are related to the geometrical/mechanical setup of the pick-up and the h, v, k and w coefficients are gains and offsets which are unknown functions of the bunch peak intensities and of the errors introduced by the electronics. Perfectly symmetric cabling and electronics, and zero offset on all 4 channels implies that $h_1 = h_2 = v_1 = v_2$ and $k_1 = k_2 = w_1 = w_2 = 0$. Furthermore, a perfectly symmetric pick-up implies that $c_{0h} = c_{0v} = c_0$, $c_{1h} = c_{1v} = c_1$ and $c_{2h} = c_{2v} = c_2$.

Under these ideal conditions, the quadrupolar moment can be derived from electrode measurements using Eq. (6):

$$R = \frac{\Sigma_\mathrm{H} - \Sigma_\mathrm{V}}{\Sigma_\mathrm{H} + \Sigma_\mathrm{V}} = \frac{c_2}{c_0} Q \tag{6}$$

where $\Sigma_\mathrm{H} = H_1 + H_2$ and $\Sigma_\mathrm{V} = V_1 + V_2$. In reality, however, the previous equation becomes more complicated and from Eqs. (2)–(5) we get:

$$R = \frac{\Sigma_\mathrm{H} - \Sigma_\mathrm{V}}{\Sigma_\mathrm{H} + \Sigma_\mathrm{V}} = \frac{A}{B} + \frac{C}{B} Q, \tag{7}$$

where:

$$\begin{aligned} A = {} & \left(h_1 + h_2\right) c_{0h} - \left(v_1 + v_2\right) c_{0v} + \\ & + \left(h_1 - h_2\right) c_{1h} x - \left(v_1 - v_2\right) c_{1v} y + \\ & + \frac{k_1 + k_2 - w_1 - w_2}{I} \end{aligned} \tag{8}$$

$$\begin{aligned} B = {} & \left(h_1 + h_2\right) c_{0h} + \left(v_1 + v_2\right) c_{0v} + \\ & + \left(h_1 - h_2\right) c_{1h} x + \left(v_1 - v_2\right) c_{1v} y + \\ & + \left(h_1 + h_2\right) c_{2h} Q - \left(v_1 + v_2\right) c_{2v} Q + \\ & + \frac{k_1 + k_2 + w_1 + w_2}{I} \end{aligned} \tag{9}$$

$$C = \left(h_1 + h_2\right) c_{2h} + \left(v_1 + v_2\right) c_{2v} \tag{10}$$

If we now plug in theoretical values for the geometric constants of typical LHC BPMs:

$$\begin{aligned} c_1 &\simeq 5 \times 10^{-2} c_0 \\ c_2 &\simeq 3 \times 10^{-3} c_0 \end{aligned} \tag{11}$$

and consider small position displacements $|x| \lesssim 1$ mm and $|y| \lesssim 1$ mm as well as values of $|Q| \lesssim 10$ mm^2 (e.g.

ISBN: 978-3-95450-204-2 ISSN: 2673-5350 doi:10.18429/JACoW-IBIC2019-TUPP034

$\sigma_H \simeq 3$ mm and $\sigma_V \simeq 1$ mm), we can simplify Eqs. (8) and (9) to write:

$$A \simeq (h_1 + h_2)\, c_{0h} - (v_1 + v_2)\, c_{0v} + + \frac{k_1 + k_2 - w_1 - w_2}{I} \quad (12)$$

$$B \simeq (h_1 + h_2)\, c_{0h} + (v_1 + v_2)\, c_{0v} + + \frac{k_1 + k_2 + w_1 + w_2}{I} \quad (13)$$

It is clear that Eq. (6) can only be used if $A \ll CQ$. In order to test this hypothesis, let us assume an asymmetry of 1% in the cancellation of the first two terms of A, thus leading to a value of $A \simeq 2 \times 10^{-2} g c_0$ without even considering the contribution of the last term. In the previous, g is the average of gains h_1, h_2, v_1 and v_2 and c_0 is the average of c_{0h} and c_{0v}. Plugging the c_2 estimate from Eq. (11) into Eq. (10), we get $CQ \simeq 4 g c_2 Q = 1.2 \times 10^{-2} g c_0 Q$. If one now takes, as a realistic example, a fairly round beam, e.g. $\sigma_H = 2.2$ mm and $\sigma_V = 2$ mm, which implies $Q \simeq Q_\sigma = 0.84$ mm^2, we would have that $CQ \simeq 10^{-2} g c_0$. Therefore, a mismatch as small as 1% in the cancellation of the first two terms of A can potentially make A twice as large as the term of interest, CQ, thus contradicting the initial hypothesis ($A \ll CQ$) and invalidating the use of Eq. (6).

Having established that Eq. (7) needs to be used to obtain the relationship between the measurement derived quantity, R, and the quadrupolar moment, Q, the next step is to obtain the multiplicative and additive constants required to calculate Q.

CALIBRATION

In the LHC, the two main instruments able to measure the transverse beam size are the WSs [6] and the synchrotron radiation telescope (SRT) [7]. The use of the WSs is limited to low intensity beams in order to prevent damage to the wire. The SRT has no such limitations since it does not interact with the beam. However, during the energy ramp, the SRT cannot provide reliable beam size measurements as the location of the radiation source is continuously changing. It is therefore of great interest to be able to use the quadrupolar moment estimated from BPM amplitudes in order to determine the transverse beam sizes during the energy ramp.

Let us take a fill for which WS scans were performed during the energy ramp. Since the transverse beam emittance $\varepsilon = \sigma^2/\beta$ is invariant along the accelerator, we can project the estimated beam sizes calculated from the WS measurements onto the positions of the BPMs by using

$$\begin{cases} \sigma^2_{\mathrm{H,BPM}} = \dfrac{\beta_{\mathrm{H,BPM}}}{\beta_{\mathrm{H,WS}}} \sigma^2_{\mathrm{H,WS}} \\ \sigma^2_{\mathrm{V,BPM}} = \dfrac{\beta_{\mathrm{V,BPM}}}{\beta_{\mathrm{V,WS}}} \sigma^2_{\mathrm{V,WS}} \end{cases} \quad (14)$$

where β is the value of the (horizontal or vertical) beta function at the WS or BPM position and σ is the corresponding transverse beam size at the same location. Due to the linear relationship found between R and Q (Eq. (7)), we can also write

$$Q_{BPM} = mR + b = \left(\sigma^2_{\mathrm{H,BPM}} - \sigma^2_{\mathrm{V,BPM}}\right) + \left(x^2_{\mathrm{BPM}} - y^2_{\mathrm{BPM}}\right) \quad (15)$$

where x and y are the measured transverse beam positions at the BPM. Having multiple wire scans, beam position measurements and R measurements, we can estimate the m ($= B/C$) and b ($= -A/C$) parameters by performing a simple linear regression.

Using the estimated parameters m and b, it is also possible to estimate the transverse beam emittances from n BPM measurements by using an appropriate optimization method for inverting the linear system

$$\begin{bmatrix} \beta_{1,\mathrm{H}} & -\beta_{1,\mathrm{V}} \\ \vdots & \vdots \\ \beta_{n,\mathrm{H}} & -\beta_{n,\mathrm{V}} \end{bmatrix} \begin{bmatrix} \varepsilon_{\mathrm{H}} \\ \varepsilon_{\mathrm{V}} \end{bmatrix} = \begin{bmatrix} m_1 R_1 + b_1 - \left(x_1^2 - y_1^2\right) \\ \vdots \\ m_n R_n + b_n - \left(x_n^2 - y_n^2\right) \end{bmatrix} \quad (16)$$

and calculate the vector of geometric emittances ε_H and ε_V. Although any number $n \geq 2$ of BPMs can be considered, the rank of the matrix of β values has to be 2. In practice, this means that we would need to include at least one BPM with dominant β_H and at least another BPM with dominant β_V.

During the energy ramp, the geometric emittance, ε, is expected to decay as $\varepsilon \sim (\beta\gamma)^{-1} \sim E^{-1}$, where in this case β is the beam velocity normalised by the speed of light, γ is the Lorentz factor and E is the beam energy. This is a direct consequence of the invariance of the normalised emittance, defined by $\varepsilon_n = \varepsilon\beta\gamma$.

RESULTS

In order to validate the method described in the previous section, we used data acquired during two energy ramps over which wire scans were performed. The beam optics are modified during the ramp to already incorporate part of the beta squeeze process that creates the optical focus at the LHC experiments. The RMS transverse beam sizes are estimated by taking the standard deviation of the Gaussian fits of the acquired beam profiles while the electrode signals used herein were taken from a set of BPMs equipped with DOROS electronics.

LHC Fill 7187

In this fill, two bunches were accelerated from 450 GeV to 6.5 TeV. A nominal bunch with 1.1×10^{11} charges and a probe bunch with approximately an order of magnitude lower intensity.

Figure 1 shows the transverse beam sizes estimated from wire scans (black curves) and projected to the location of different BPMs using Eq. (14). From the vertical beam size (bottom plot of Fig. 1) we can see the expected $\varepsilon \sim \sigma^2 \sim (\beta\gamma)^{-1} \sim E^{-1}$ behaviour mentioned previously. Unfortunately, profile data acquired during some of the horizontal scans was saturated. This fact, as well

ISBN: 978-3-95450-204-2 ISSN: 2673-5350 doi:10.18429/JACoW-IBIC2019-TUPP034

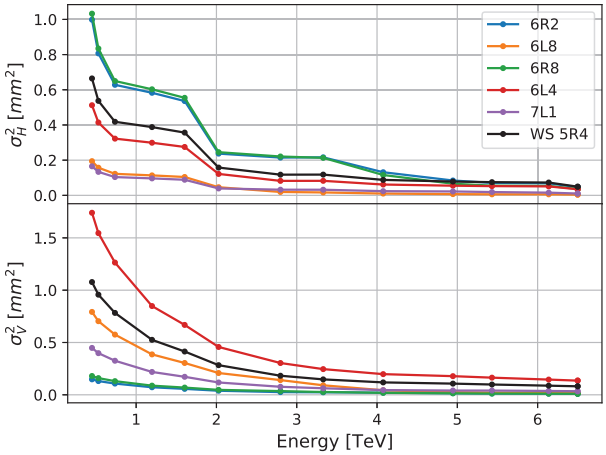

Figure 1: LHC fill 7187 - transverse beam sizes.

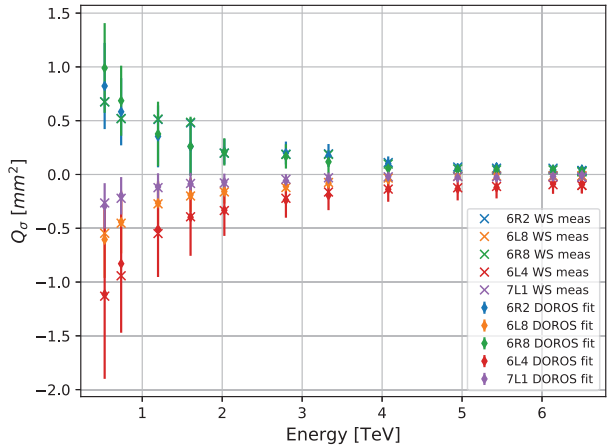

Figure 2: Q_σ fit results.

as potential uncertainties in the knowledge of the true beta function, can explain the observed deviations from the expected $\sigma^2 \sim E^{-1}$ behaviour in some points of the top plot of Fig. 1. We will use this experimental data, nevertheless.

Let us now take BPM measurements R, x and y, and fit Eq. (17) in order to extract both the m and b parameters.

$$Q_\sigma = mR + b - \left(x^2 - y^2\right) \tag{17}$$

In this equation, Q_σ represents the beam size contribution to the quadrupolar moment projected to the location of the different BPMs and is calculated from the closest pair of horizontal and vertical wire scans. R is calculated from the BPM electrode amplitudes as described in Eq. (6) and x and y are the average beam positions[1].

The results are shown in Fig. 2, where the crosses represent the Q_σ measured from wire scans and the dots (along with the corresponding confidence interval) represent what is obtained from the BPM electrode amplitudes after the fit. 10% statistical errors (1σ) are assumed for the values of the beta functions, position measurements and WS beam size estimations. It is consistent, from the monotonicity of the points in Fig. 2, that at the location of the 6R2 and 6R8 BPMs the horizontal beta function dominates whereas elsewhere the vertical beta function dominates. Overall, there is an agreement between the fitted BPM data and the WS data. A poorer agreement on the 3rd and 4th scans can be observed for the BPMs for which the horizontal beta function dominates (i.e. 6R2 and 6R8). The absolute decrease in the span of the confidence interval, also visible in Fig. 2, is due to the decrease in beam size.

Table 1 shows the values of the fitted parameters, as well as their 1σ relative errors. From Eqs. (7) and (17) we have that $m = B/C$ and $b = -A/C$.

Having estimated m and b for each BPM, we can now solve the linear system of Eq. (16) by applying a standard least-square fitting method and calculate the vector of geometric emittances using only BPM data. Figure 3 shows a comparison between the normalised emittances calculated via this method with the normalised emittances estimated from the individual wire scans. In the case of the vertical emittance, there is a good agreement between this method and the WS scans throughout the ramp. In the case of the horizontal emittance, the agreement is in general poorer.

Table 1: BPM Q Calibration

BPM	m	$\frac{\sigma_m}{m}$	b	$\frac{\sigma_b}{b}$
6R2	248.11	0.11	-0.79	-0.12
6L8	239.24	0.06	0.2	0.05
6R8	320.77	0.11	0.71	0.10
6L4	371.46	0.05	-0.22	-0.02
7L1	270.22	0.08	-0.2	-0.07

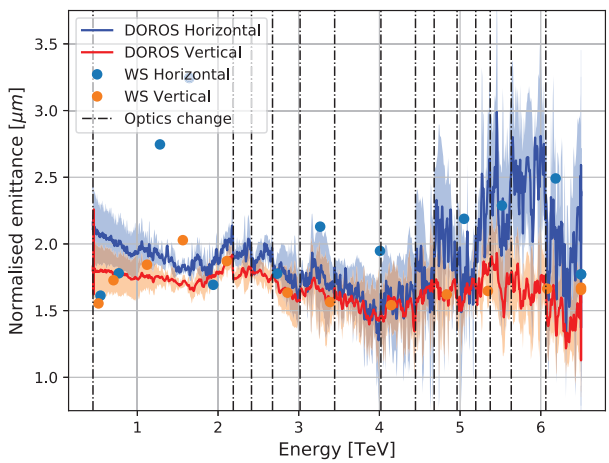

Figure 3: Normalised emittance.

[1] R, x and y are calculated from taking the electrode signal samples at the mean time between the most simultaneous pair of horizontal and vertical wire scans.

ISBN: 978-3-95450-204-2 ISSN: 2673-5350 doi:10.18429/JACoW-IBIC2019-TUPP034

LHC Fill 7220

In this fill, 13 nominal bunches were accelerated from 450 GeV to 6.5 TeV. These bunches, of similar intensity, added up to a total beam intensity of 1.1×10^{12} charges. The same analysis was carried for this data with the results summarised in Table 2 and plotted in Figs. 4 and 5.

The results from the BPM measurements in this case again agree rather well with that from the wire scans with better agreement in the vertical plane than the horizontal.

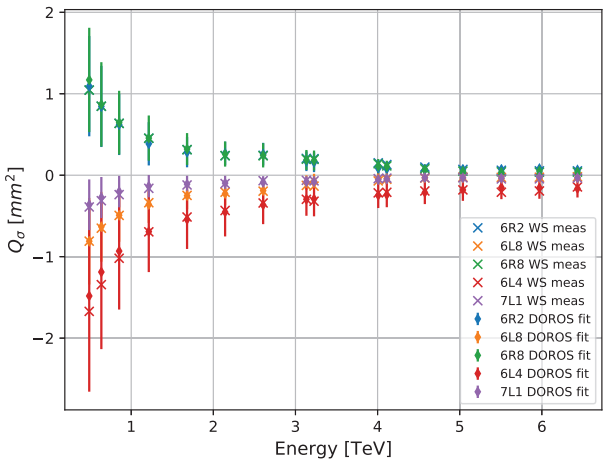

Figure 4: Q_σ fit results.

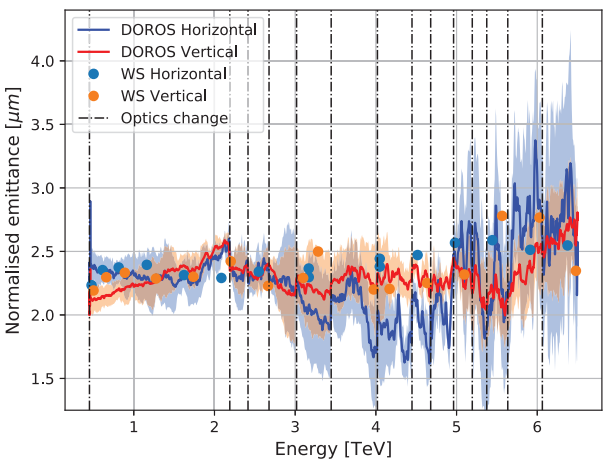

Figure 5: Normalised emittance.

Table 2: BPM Q Calibration

BPM	m	$\frac{\sigma_m}{m}$	b	$\frac{\sigma_b}{b}$
6R2	439.15	0.11	-2.1	-0.11
6L8	442.64	0.07	-0.87	-0.08
6R8	437.95	0.03	-0.094	-0.07
6L4	647.10	0.07	-0.99	-0.05
7L1	444.99	0.08	-1.2	-0.07

DISCUSSION AND CONCLUSIONS

As observed in Figs. 2 and 4, Eq. (17) seems to describe well the overall $Q(R)$ relationship, keeping in mind as previously discussed, that some horizontal scans performed during the ramp of fill 7187 provided biased estimations of the normalised emittance. Furthermore, since the horizontal and vertical scans are not simultaneous, there is a deterioration in the accuracy of the WS-based Q_σ estimations, thus making the times at which matching samples are selected from the BPM electrode amplitudes an average between the time of the two scans.

It is interesting to note, from Table 2, that all BPMs except 6L4 have similar m values. This is consistent with the fact that all except 6L4 have a button size of 24 mm and an aperture of 49 mm whereas 6L4 has a button size of 34 mm and an aperture of 61 mm. In Table 1 this is less evident for the 6R8 and 7L1 BPMs. We also notice that the $m = B/C$ values for the same BPMs in both tables differ by a factor of $\approx$ 1.7. Assuming that the rightmost offset term of Eq. (13) is fairly random from BPM to BPM, then this difference can only be explained by differences in the discrepancies between the horizontal and vertical gains and geometric constants.

The final calculations of the normalised emittances, as shown in Figs. 3 and 5, reveal a good agreement in the vertical plane and a poorer agreement in the horizontal plane. Further studies are ongoing in order to understand this discrepancy. Furthermore, the abrupt jumps in the traces at the time of optics changes point to an uncertainty of the beta functions as it is unlikely that the emittance itself could change that fast, and can certainly never reduce.

In typical LHC physics fills it is not possible to use wire scans during the ramp. Since the gains of the DOROS electronics are sensitive to the bunch peak intensities, we can devise a scenario where the electronic settings of a typical physics ramp are used in a special calibration fill with a few bunches of similar bunch peak intensity, thus allowing wire scans for performing the cross calibration. From then onward, it is hoped that the same calibration can be used for subsequent physics fills without the need to frequently cross-calibrate the system.

ACKNOWLEDGEMENTS

The authors would like to kindly acknowledge the work of J. Olexa and A. Sounas and the assistance of G. Azzopardi.

REFERENCES

[1] J. Olexa and M. Gasior, "Synchronisation of the LHC Betatron Coupling and Phase Advance Measurement System", in *Proc. IBIC'14*, Monterey, CA, USA, Sep. 2014, paper MOPD04, pp. 139–143.

[2] J. Olexa, "Design and Optimization of the Beam Orbit and Oscillation Measurement System for the Large Hadron Collider", Ph.D. thesis, Slovak Tech. U., Bratislava, Slovakia, Rep. CERN-THESIS-2018-185, 2018.

ISBN: 978-3-95450-204-2 ISSN: 2673-5350 doi:10.18429/JACoW-IBIC2019-TUPP034

[3] A. Sounas *et al.*, "Beam Size Measurements Based on Movable Quadrupolar Pick-ups", in *Proc. IPAC'18*, Vancouver, Canada, Apr.-May 2018, pp. 2028–2031. doi:10.18429/JACoW-IPAC2018-WEPAF080

[4] A. Sounas, M. Gasior, and T. Lefevre, "BPM Technologies for Quadrupolar Moment Measurements", in *Proc. HB'18*, Daejeon, Korea, Jun. 2018, pp. 399–403. doi:10.18429/JACoW-HB2018-THA1WE03

[5] T. Suwada, "Multipole Analysis of Electromagnetic Field Generated by Single-Bunch Electron Beams", *Japanese Journal of Applied Physics*, vol. 40, pp. 890–897, 2001. doi:10.1143/jjap.40.890

[6] J. Bosser and C. Bovet, "Wire scanners for LHC", CERN, Geneva, Switzerland, Rep. CERN-LHCProject-Note-108, Sep 1997.

[7] A. Goldblatt, E. Bravin, F. Roncarolo, and G. Trad, "Design and Performance of the Upgraded LHC Synchrotron Light Monitor", CERN, Geneva, Switzerland, Rep. CERN-ACC-2013-0300, Sep 2013.